Micro and Nano Systems Letters

LETTER

Open Access

# 3D printing fabrication process for fine control of microneedle shape

Jinwoong Jeong, Jaeu Park and Sanghoon Lee*

**Abstract**

Microneedle electrode (ME) is used to monitor bioelectrical signals by penetrating via the skin, and it compensates for a limitation of surface electrodes. However, existing fabrication of ME have limited in controlling the shape of microneedles, which is directly relevant to the performance and durability of microneedles as an electrode. In this study, a novel method using 3D printing is developed to control needle bevel angles. By controlling the angle of printing direction, needle bevel angles are changed. Various angles of printing direction (0–90°) are investigated to fabricate moldings, and those moldings are used for microneedle fabrications using biocompatible polyimide (PI). The height implementation rate and aspect ratio are also investigated to optimize PI microneedles. The penetration test of the fabricated microneedles is conducted in porcine skin. The PI microneedle of 1000 μm fabricated by the printing angle of 40° showed the bevel angle of 54.5°, which can penetrate the porcine skin. The result demonstrates that this suggested fabrication can be applied using various polymeric materials to optimize microneedle shape.

**Keywords:** Microneedle electrode, 3D printing, Polyimide microneedle, Needle-shape control

## Introduction

Bioelectrical signals are important physiological parameters that allow to analyze the state and information of the body. The most common method to monitor bioelectrical signals like electromyogram (EMG) is to attach surface electrodes (SE) on the skin. The microneedle electrode (ME) is an invasive dry electrode penetrating stratum corneum of the skin with a needle, so recording quality is improved compared with SE. In the current ME fabrication process, various methods such as etching [1–7], photolithography [7, 8], molding [9–13], magnetorheological drawing lithography [14, 15], thermal drawing [16], laser machining [17–22], electrical discharge machining [23, 24], and various other methods have been developed. These methods allow designing length or aspect ratio of microneedles freely, making it possible to create an optimal design. However, most fabrication processes require expensive facilities and multiple fabrications steps.

In addition, the material of the microneedle is also important. Currently, various types of materials are used for microneedles, such as rigid materials [17, 20], polymer [4, 12], and silicon [5, 6]. Skin penetration of microneedle requires stiff materials. However, there is a risk of microneedle breakage after implantation inside the skin that causes various side effects.

Accordingly, biocompatible and flexible materials such as polymer are preferred to fabricate microneedle. Polymer-based microneedles are mainly manufactured by molding fabrication. There are many ways to make a microneedle mold. Recently, it is possible to develop more sophisticated and complex microneedles using polymer materials at an inexpensive cost through the molding fabrication process using 3D printing [14]. Currently, various mechanisms have been developed for 3D printing, such as FDM (Fused Deposition Modeling), DLP (Digital Light Processing), SLA (Stereo Lithography Apparatus), etc. In this study, the SLA printing

*Correspondence: hoonw@dgist.ac.kr

Department of Robotics and Mechatronics Engineering, Daegu Gyeongbuk Institute of Science and Technology (DGIST), 333, Techno Jungang-Daero, Hyeonpung-Eup, Dalseong-Gun, Daegu 42988, Republic of Korea

method was used to fabricate a 3D printed microneedle mold. SLA printing uses a laser to harden a photocurable resin. A laser is fired at the resin tank to harden the resin to form one layer, and the next layer is stacked on the layer. Currently, the SLA printing method is widely used because it is relatively inexpensive and allows for sophisticated printing. However, there is a limit to the resolution because the resolution of the output is determined by the size of the laser. Since the SLA printer operates with the same mechanism as in Fig. 1a, it is unable to express a layer smaller than the laser size. As a result of these mechanisms, the design and output results are different due to the limitation of the resolution of the 3D printer when printing delicate and small objects such as microneedles.

In this study, in order to reduce the effect of microneedles on the human body after insertion into the skin, the microneedle was fabricated using a polymer rather than a rigid object such as metal. However, polymer materials typically have low mechanical strength, causing break during the penetration. Therefore, the optimization of polymer microneedle in terms of shapes, length,

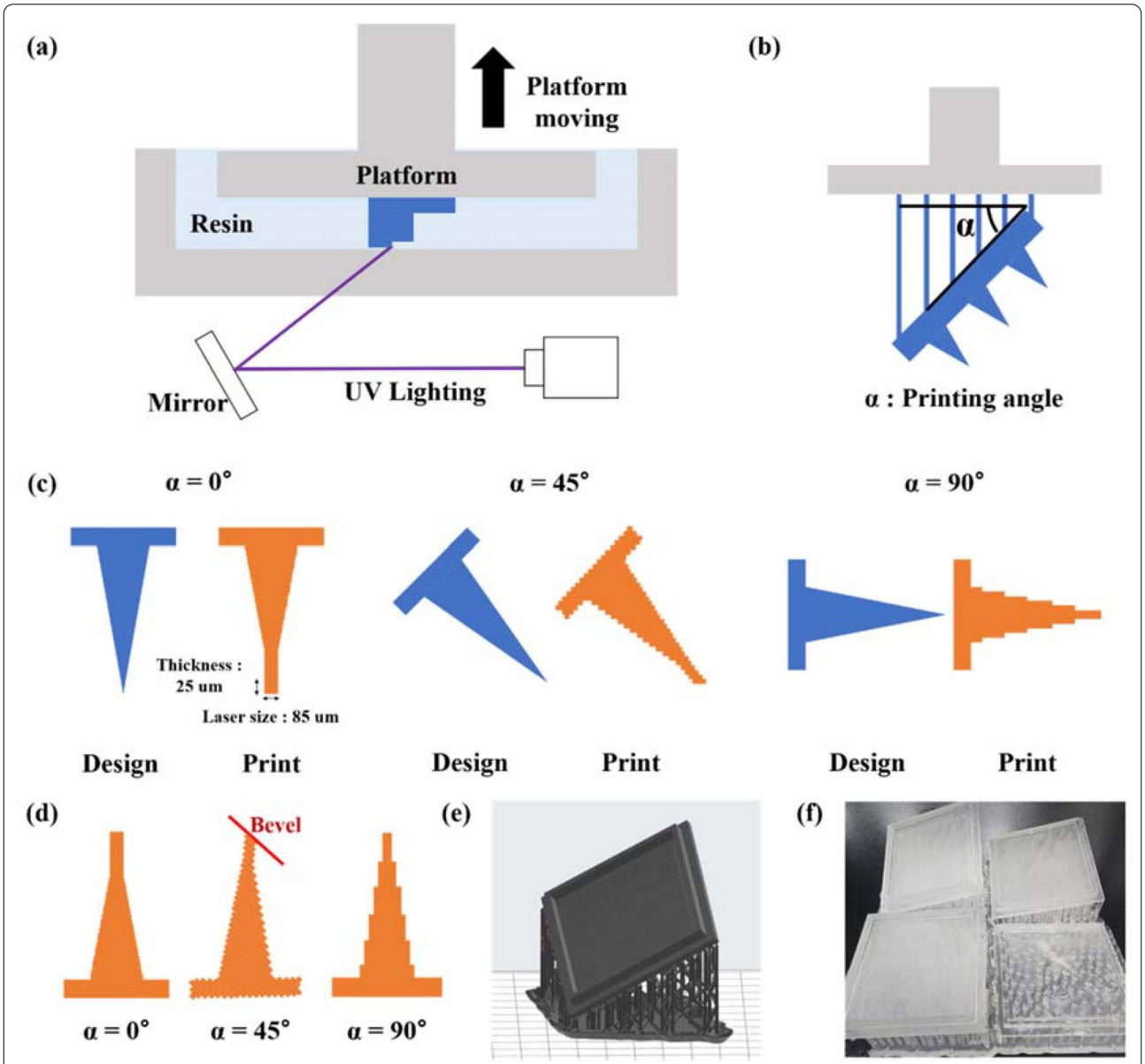


**Fig. 1** **a** The schematic diagram of SLA 3D printing. **b** The schematic diagram of 3D printing angle setting. **c**–**d** The schematic diagrams of original design and printed microneedles according to printing angles. **e** An image of 3D printing setting at the angle of 45°. **f** Printed molds (0–30°)

and bevel angles is required to maximize the penetration capacity. In particular, the bevel of the microneedle tip reduces the insertion force required to penetrate the stratum corneum of the skin, thereby reducing pain and the possibility of breakage of the microneedle [7, 21, 22].

However, there are some limitations to use polymer microneedle as an electrode**.** The first is the durability of microneedles including during and after implantation. The second one is that it is difficult to control the shape of microneedles including needle bevel which is directly relevant to penetration capability, secure after implantation, and tissue damage. The current 3D printing fabrication requires a new method because it is difficult to satisfy these requirements due to the limitation of resolution. But despite several attempts, an effective process to control microneedle shape using soft and biocompatible materials has not been developed.

In this study, we propose a novel 3D printing fabrication process that enables to control microneedle bevel angles of polyimide (PI) microneedles. Polyimide (PI) has excellent biocompatibility [25] and excellent adhesion to metals. This allows to provide minimally invasive penetration on the skin thanks to relatively soft materials when it maximizes its penetration capability. To maximize the penetration of PI microneedles, microneedle bevel angles were changed by changing a printing angle of SLA printer from 0 to 90° as shown in Fig. 1b. Due to the limitations of the 3D print resolution, delicate microneedle tips are unable to fabricate using the normal method ($\alpha = 0°$) while the printing angle changes to provide different bevel angles (Fig. 1c, d). Furthermore, aspect ratio and achievable height of the PI microneedle were investigated with various lengths (100 to 1000 μm). Finally, a penetration test of the fabricated PI microneedle via porcine skin was conducted to find the optimized condition.

## Materials and methods

### 3D printing microelectrode fabrication

A corn shape of microneedles was designed using AutoCAD 2020, then was printed by using a 3D Form 3 printer (FormLabs, Somerville, Massachusetts) with different printing angles (α) of from 0 to 90° (10° step). The height of microneedles was also changed from 100 to 1000 μm to investigate height implementation rate from design to fabricated output as well as aspect ratio of the fabricated microneedles. For the first molding process, the 3D printed mold was design to form PDMS mold. PDMS was then poured into the printed mold, and formed the final PDMS mold. After that, PI was poured into the PDMS mold, and then placed in a vacuum chamber -1 atm for 10 min to remove bubbles as well as to fill the PI into the narrow vacancy of needle pattern at mold. Curing was performed by exposing a UV light (405 nm) to PI, and hard baking (200 °C for 1 h) was performed. Finally, the microneedle was removed from the PDMS mold (Fig. 2a). Figure 2b shows the picture of the fabricated PI microneedle.

### Microneedle characteristics

The fabricated microneedle was investigated using SEM to analyze the shape, length, and bevel angle of the fabricated microneedle. Furthermore, the insertion test of the fabricated PI microneedle was conducted in porcine skin that has similar characteristics to human skin [26]. The force required to penetrate the porcine skin at a speed of 0.1 mm/sec was obtained. Insertion test was conducted by MultiTest 2.5-i (Mecmesin, Slinfold, UK) (Fig. 2c).

## Results and discussion

### 3D Printed Polyimide Microneedle

Figure 3a shows the shape of microneedles that were designed using the AutoCAD 2020. The printed 3D microneedles depending on the printing angles were shown in Fig. 3b. The SLA printing is a method of curing photocurable resin by a laser, so the width of the stacked layers varies depending on the printing angles (Fig. 1c). Therefore, the smaller size of sharp tips less than the size of laser cannot be printed. As expected, the flat tip was formed at the angle (α) of 0° which is a normal printing angle. And slightly tilted bevel was formed when the angle increased. As shown in Fig. 3b, the needle bevel angle was formed from the angles were between 10 and 60°, while the angles were slightly collapsed after the higher angles more than 70° due to the gravity. Above the printing angle of 70°, the needle bent toward the floor. This result indicates that a certain level of printing angles allows controlling microneedle bevel angles.

With the molding process, PI microneedles were fabricated using the printed microneedles. As shown in Fig. 3c, the needle bevel angles of the fabricated PI microneedle were changed depending on the different conditions. The similar result from the printed microneedle was observed in that the printing angle (α) from 20 to 50° formed needle bevel angles at the PI microneedle tips. The printing angle of 10° shows a very small angle, and angles above 50° appear uncontrollable.

To analyze printing controllability using this fabrication method, the bevel angle of the 3D printed microneedle was defined as β, and the bevel angle of the fabricated PI microneedle was defined as γ as shown in Fig. 4a. Figure 4b shows the bevel angle result of the printed 3D microneedle and the fabricated PI microneedle depending on the printing angles. Theoretically, β has a similar value calculated as '90°-α', but above the certain angle, it varies since it is affected by the gravity. Overall results

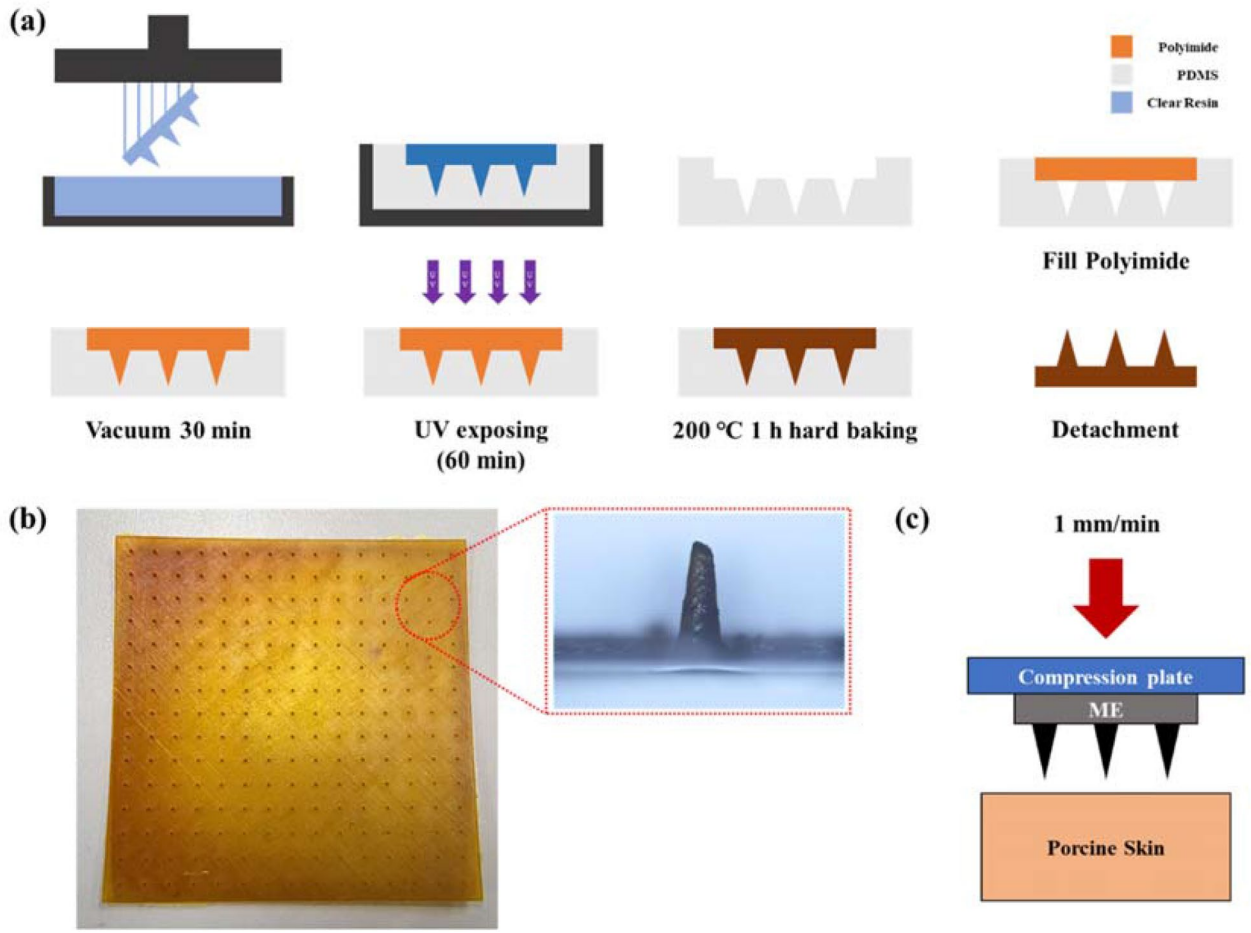


**Fig. 2** **a** Fabrication process of polyimide microneedle. **b** The fabricated PI microneedles. **c** The schematic diagram of insertion test

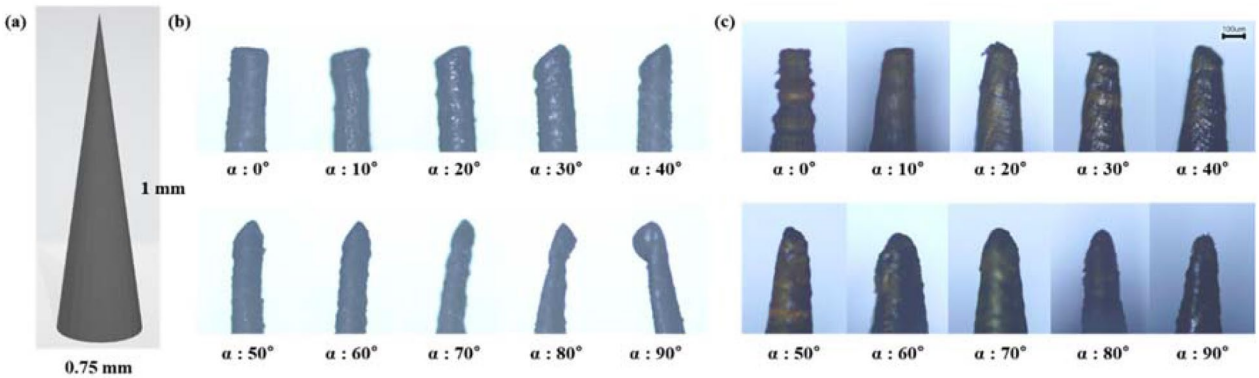


**Fig. 3** **a** AutoCAD design. **b** Pictures of 3D printed microneedles at the angle setting from 0 to 90°. **c** Pictures of polyimide (PI) microneedles at the angle setting from 0 to 90°

of the bevel angles (β) were quite matched well to the expected values within the ranges of the angles from 0 to 40°, and the printed PI microneedle bevel angles (γ) were slightly larger than the 3D print microneedle bevel angle (β). The sharpest bevel angle was 54.5° that was fabricated by the angle (α) at 40°. However, after the angle (α) of 40°,

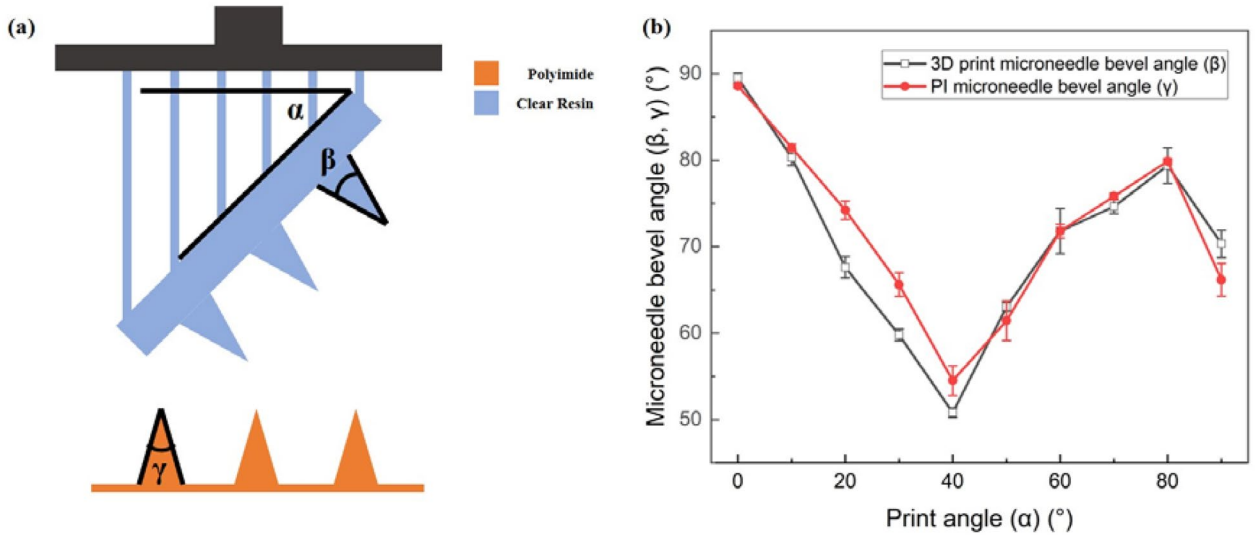


**Fig. 4** **a** The schematic diagram of 3D printed microneedle and PI microneedle. **b** The bevel angle of the microneedle according to the print angle. (α: printing angle, β: 3D printed microneedle bevel angle, γ: PI microneedle bevel angle) (n = 10)

the bevel angle tends to increase again, and was uncontrollable above the angle of 60°. When α is 90°, the bevel angle decreases again, which seems to be a phenomenon caused the distorted shape of the printed microneedle tip as shown in Fig. 3b. The detailed data is summarized in Table 1.

The results indicate that the change of printing angle (α) allows controlling the bevel angles (β) within the certain ranges (50.8–89.5°) as well as the followed molding process using this angle-controlled microneedle enables to control the bevel angle (γ) of the fabricated PI microneedles within the certain ranges (54.5–88.6°). The sharpest angle (γ) of 50° was achieved using this process.

### Height dependent aspect ratio

For microneedles, aspect ratio and height are also important parameters. To investigate the aspect ratio according to the print height, the microneedle with

**Table 1** Fabrication of microneedle

| Method | Materials | Advantages | Limits | Refs. |
|---|---|---|---|---|
| Etching | Silicon, Polymer | High aspect ratio, Suitable for mass production | Expensive, Complex fabrication process, Low durability | [1–7] |
| Photolithography | Polymer | High aspect ratio, Suitable for mass production | Expensive, Complex fabrication process, Low durability | [7, 8] |
| Molding | Metal, Polymer | Suitable for mass production, High reproducibility, Various microneedle forms can be implemented | Complex fabrication process, Low durability | [9–13] |
| Magnetorheological drawing lithography | Polymer | High aspect ratio, Simple fabrication process, Suitable for mass production | Rough surface, Low durability | [14, 15] |
| Thermal drawing | Polymer | High aspect ratio, Simple fabrication process, Suitable for mass production | Low reproducibility, Low durability | [16] |
| Laser machining | Metal | Simple fabrication process | Blunt microneedle tip, Rough surface, Low biocompatibility | [17–22] |
| Electrical discharge machining | Metal | High aspect ratio, High reproducibility | Expensive, Complex fabrication process | [23, 24] |
| 3D print double molding | Polymer | Suitable for mass production, High reproducibility, Various microneedle forms can be implemented, Bevel angle control, Simple fabrication process | Resolution limit, Low durability, Rough surface | This paper |

aspect ratio of 4 was designed with the height change from 100 to 1000 μm. And the designed microneedle was fabricated. The microneedles with a height of 100 μm were not fabricated properly due to very short of the height. Figure 5a shows the aspect ratio results of the fabricated PI microneedle (with all α values) according to the printing height. The aspect ratio was 0.78 (n = 10) when the height was 200 μm that shows quite poor aspect ratio. As the height was increased, the aspect ratio was also increased, and showed the highest value of 2.58 (n = 10) when the height was 1000 μm. The aspect ratio of commonly used microneedles is 2:1 or higher [27, 28], therefore, the fabricated PI microneedles longer than the height of 600 μm can be used (Fig. 6).

Height implementation rate of designed and fabricated height was measured and calculated. As shown in Fig. 5b, the print height affects the height implementation rate of the PI microneedle. When the input print height was 200 μm, the height implementation rate of the fabricated PI microneedle was only 71.6%, but this rate increased as the print height increased. The height implementation rate showed 90.9% when the input print height was 800 μm, and it was reached the maximum value of 92.6% when the input print height was 900 μm. When the print height was 1000 μm, it slightly decreased to 91.6%, but

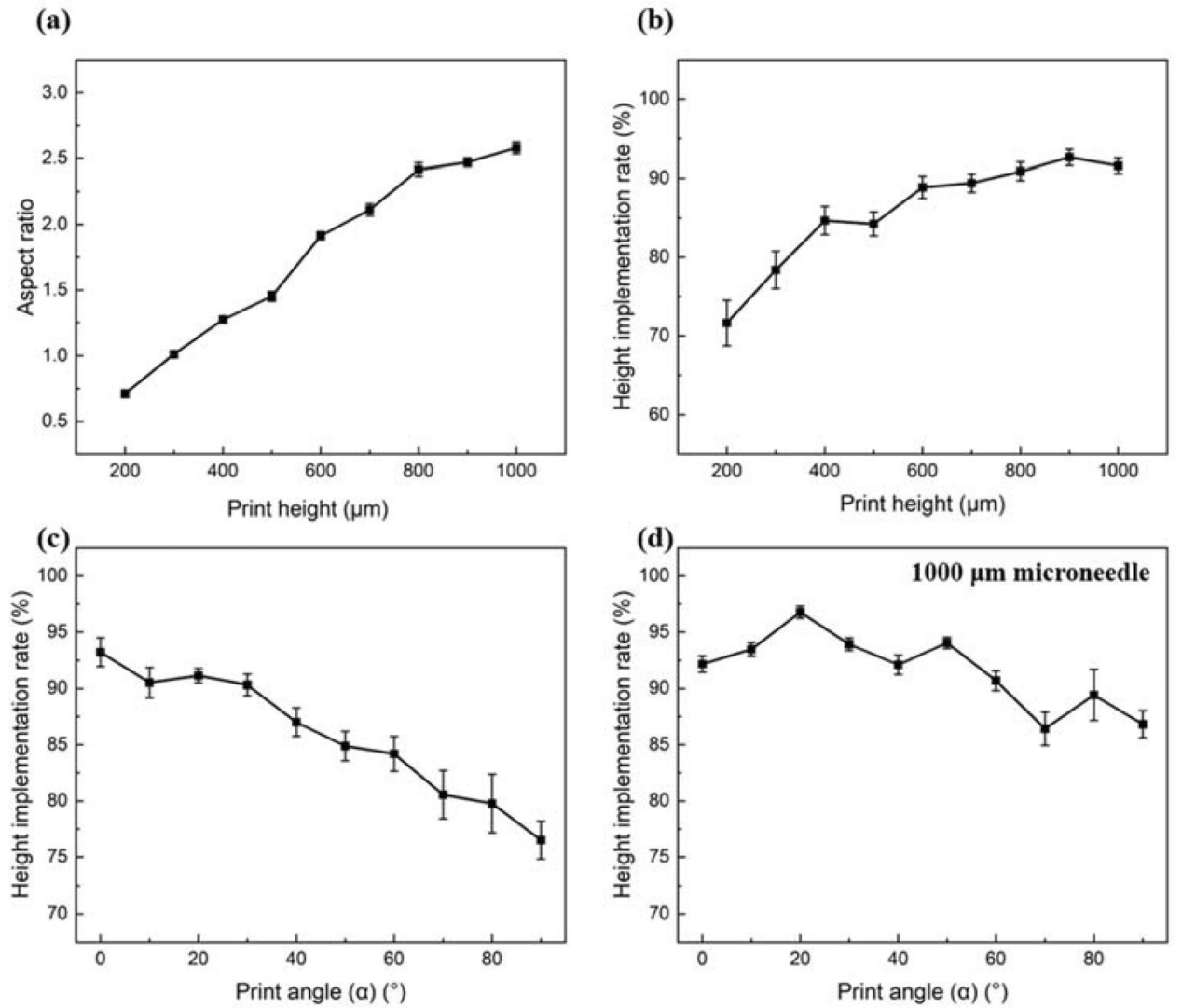


**Fig. 5** **a** The result of aspect ratio of PI microneedles according to the print height (n = 10). **b** The result of height implementation rate of the PI microneedle according to the print height (n = 10). **c** The result of height implementation rate of the PI microneedle (all heights) according to the print angle (n = 10). **d** The result of height implementation rate of the PI microneedle (1000 μm) according to the print angle (n = 10)

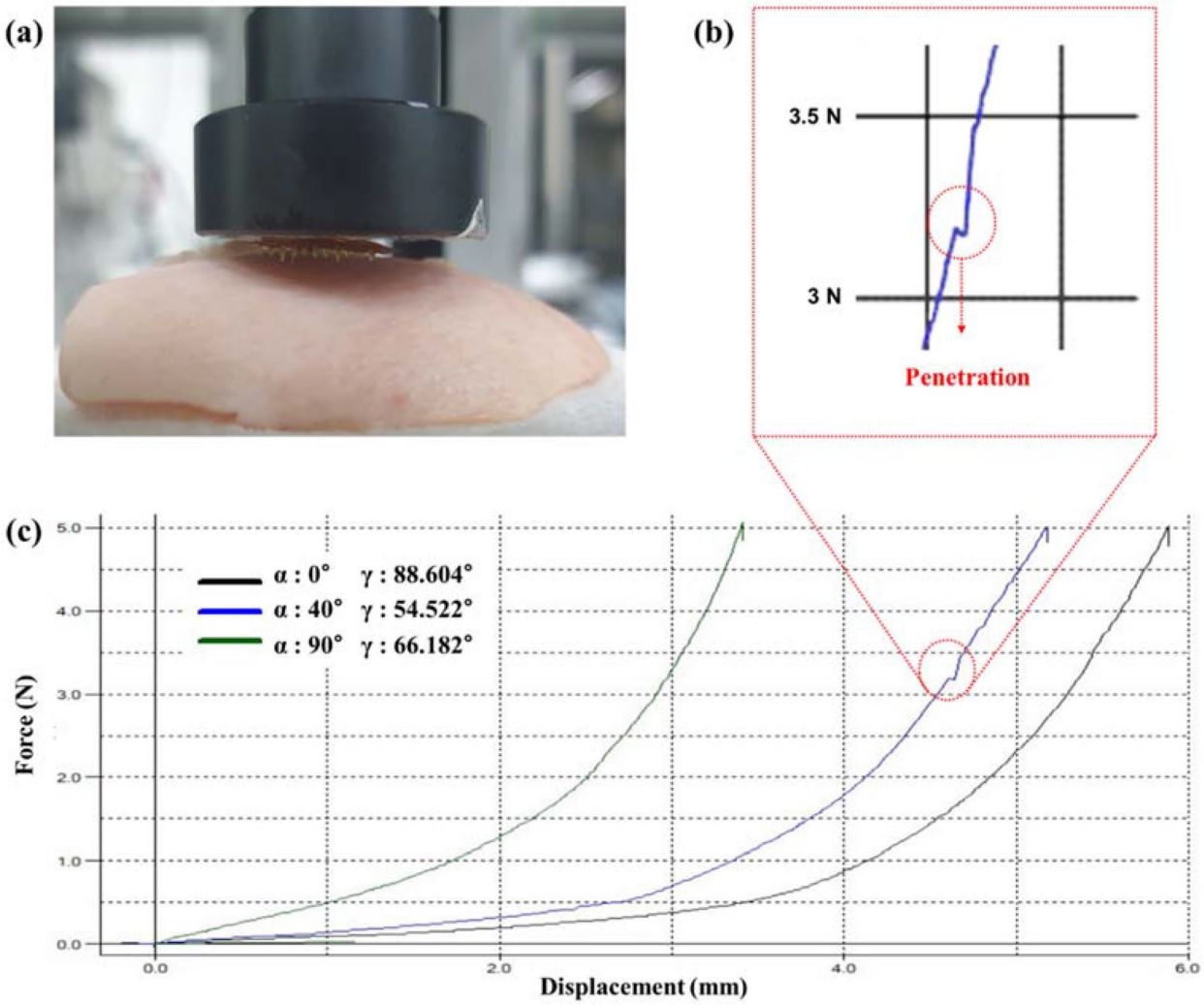


**Fig. 6** **a** The picture of penetration test. **b** The results of penetration test in porcine skins

the decrease can be negligible. In addition, it is shown that the error bar (standard error of mean) in Fig. 5b decreases as the print height increases, which indicate that the longer PI microneedle can be fabricated uniformly. The detailed data is summarized in Table 2.

Figure 5c shows the height implementation rate of the fabricated PI microneedle (all heights) according to the print angle (α). Overall, as the print angle increased, the height implementation rate decreased. When α was 0°, the height implementation rate was 93.2%, which is the maximum value, while when α was 90°, it decreased to 76.5%. When α was 40°, where showed the sharpest bevel angle of the PI microneedle, the height implementation rate was 87.0%.

Figure 5d shows the height implementation rate of the fabricated PI microneedle (with the print height of 1000 μm) according to the print angle (α). When α was 20°, the height implementation rate of the fabricated PI microneedle was 96.8%, which is the maximum value. When α was 70°, the minimum value of 86.4% was obtained. When α was 40°, the height implementation rate was 92.1%. This value is quite good and indicates that the PI microneedle fabricated with the print angle (α) of 40° and the print height of 1000 μm is recommended. Figure 5c, d, the error bar of the graph decreased slightly as the print angle (α) increases till α was 30°, but it increased after that, which indicate that as the print angle increases more than 30°, the implementation of the bevel part of the microneedle becomes non-uniform.

### Penetration of porcine skin

Penetration test through porcine skin was conducted using the fabricated PI microneedle of 1000 μm height depending on the printing angle (α) of 0°, 40°, and 90°. As shown

**Table 2** The results of 3D printed microneedle bevel angle (β) and PI microneedle bevel angles (γ) depending on printing angle (α)

| Print angle (α) | 3d print microneedle tip angle (β) | Stand Error of Mean (β) | PI microneedle tip angle (γ) | Stand Error of Mean (γ) |
|---|---|---|---|---|
| 0 | 89.510 | 0.587 | 88.604 | 0.219 |
| 10 | 80.304 | 0.902 | 81.452 | 0.414 |
| 20 | 67.624 | 1.216 | 74.220 | 1.061 |
| 30 | 59.802 | 0.681 | 65.628 | 1.352 |
| 40 | 50.804 | 0.542 | 54.522 | 1.696 |
| 50 | 63.070 | 0.505 | 61.456 | 2.285 |
| 60 | 71.796 | 2.610 | 71.790 | 0.809 |
| 70 | 74.620 | 0.789 | 75.817 | 0.352 |
| 80 | 79.380 | 2.062 | 79.879 | 0.329 |
| 90 | 70.318 | 1.580 | 66.182 | 1.874 |

in Fig. 6, PI microneedle fabricated by the printing angle (α) of 0° which is the normal printing condition shows stable pushing performance, but unable to penetrate the skin. PI microneedle fabricated by the printing angle (α) of 90° shows poor performance and break quickly due to the unstable shape. The penetration was only observed with the PI microneedle fabricated by the printing angle (α) of 40°. This result demonstrates that PI microneedle of 1000 μm height (aspect ratio: 2.58) fabricated by the printing angle (α) of 40° has the maximized penetration capability.

## Conclusion

We suggested a novel fabrication process to control microneedle bevel angles using polymeric materials. To validate this process, biocompatible polyimide (PI) was used as microneedle materials, and the PI microneedle was fabricated and optimized to maximize its penetration capability. By changing the printing angle (α) of current 3D printer that have resolution limitation, the microneedle bevel angle could be changed which is critical for penetration function of microneedles. The microneedle bevel angles, aspect ratio, and height implementation ratio of 3D printed microneedles and PI microneedles fabricated by the molding process were compared to optimize the PI microneedle. Finally, penetration test of porcine skin was demonstrated to evaluate the penetration capability. The PI microneedle of 1000 μm (the aspect ratio: 2.58) fabricated by the printing angle (α) of 40° (γ: 54.52) has the maximized penetration capability. We expect that this fabrication process can also apply to other polymeric materials allowing the control of microneedle shape and bevel angle.

## Rights and permissions



### Author contributions

JJW designed and conducted the overall experiment. He also analyzed the data. PJW assisted in the PI microneedle fabrication process. LSH supervised this research, evaluated and edited the manuscript. All authors read and approved the final manuscript.

### Funding

This research was supported by a Korea Medical Device Development Fund grant funded by the Korea government (the Ministry of Science and ICT, the Ministry of Trade, Industry and Energy, the Ministry of Health & Welfare, the Ministry of Food and Drug Safety) (Project Number: 1711135031, KMDF_PR_20200901_0158-05).

### Availability of data and materials

All data generated or analyzed during this study are included in this published article.

## Declarations

### Ethics approval and consent to participate

The authors declare that they have no competing interests.

### Consent for publication

Authors consent the SpringerOpen license agreement to publish the article.

### Competing interests

The authors declare that they have no competing interests.

Received: 8 September 2022 Accepted: 7 December 2022
Published online: 02 January 2023

**References**

1. Wilke N, Mulcahy A, Ye S-R, Morrissey A (2005) Process optimization and characterization of silicon microneedles fabricated by wet etch technology. Microelectron J 36(7):650–656
2. Roxhed N, Griss P, Stemme G (2007) A method for tapered deep reactive ion etching using a modified Bosch process. J Micromech Microeng 17(5):1087
3. Roh H, Yoon YJ, Park JS, Kang DH, Kwak SM, Lee BC, Im M (2022) Fabrication of high-density out-of-plane microneedle arrays with various heights and diverse cross-sectional shapes. Nano-Micro Lett 14(1):1–19
4. Wang R, Jiang X, Wang W, Li Z (2017) A microneedle electrode array on flexible substrate for long-term EEG monitoring. Sens Actuators, B Chem 244:750–758
5. Wei-Ze L, Mei-Rong H, Jian-Ping Z, Yong-Qiang Z, Bao-Hua H, Ting L, Yong Z (2010) Super-short solid silicon microneedles for transdermal drug delivery applications. Int J Pharm 389(1–2):122–129
6. Pradeep Narayanan S, Raghavan S (2019) Fabrication and characterization of gold-coated solid silicon microneedles with improved biocompatibility. Int J Adv Manuf Technol 104(9):3327–3333
7. Khanna P, Luongo K, Strom JA, Bhansali S (2010) Sharpening of hollow silicon microneedles to reduce skin penetration force. J Micromech Microeng 20(4):045011
8. Takahashi H, Jung Heo Y, Arakawa N, Kan T, Matsumoto K, Kawano R, Shimoyama I (2016) Scalable fabrication of microneedle arrays via spatially controlled UV exposure. Microsyst Nanoeng 2:16049. https://doi.org/10.1038/micronano.2016.49
9. Ng W, Seet H, Lee K, Ning N, Tai W, Sutedja M, Fuh J, Li X (2009) Microspike EEG electrode and the vacuum-casting technology for mass production. J Mater Process Technol 209(9):4434–4438
10. Arai M, Nishinaka Y, Miki N (2015). Long-term electroencephalogram measurement using polymer-based dry microneedle electrode. 2015 Transducers-2015 18th International Conference on Solid-State Sensors, Actuators and Microsystems (TRANSDUCERS)
11. Mahmood M, Kwon S, Kim H, Kim YS, Siriaraya P, Choi J et al (2021) Wireless soft scalp electronics and virtual reality system for motor imagery-based brain-machine interfaces. Adv Sci 8(19):2101129
12. Sullivan SP, Koutsonanos DG, del Pilar Martin M, Lee JW, Zarnitsyn V, Choi SO et al (2010) Dissolving polymer microneedle patches for influenza vaccination. Nat Med 16(8):915–920
13. Krieger KJ, Bertollo N, Dangol M, Sheridan JT, Lowery MM, O'Cearbhaill ED (2019) Simple and customizable method for fabrication of high-aspect ratio microneedle molds using low-cost 3D printing. Microsyst Nanoeng 5:42. https://doi.org/10.1038/s41378-019-0088-8
14. Chen Z, Ren L, Li J, Yao L, Chen Y, Liu B, Jiang L (2018) Rapid fabrication of microneedles using magnetorheological drawing lithography. Acta Biomater 65:283–291. https://doi.org/10.1016/j.actbio.2017.10.030
15. Chen Z, Ye R, Yang J, Lin Y, Lee W, Li J, Ren L, Liu B, Jiang L (2019) Rapidly fabricated microneedle arrays using magnetorheological drawing lithography for transdermal drug delivery. ACS Biomater Sci Eng 5(10):5506–5513. https://doi.org/10.1021/acsbiomaterials.9b00919
16. Ren L, Jiang Q, Chen K, Chen Z, Pan C, Jiang L (2016) Fabrication of a micro-needle array electrode by thermal drawing for bio-signals monitoring. Sensors 16(6):908
17. Guvanasen GS, Guo L, Aguilar RJ, Cheek AL, Shafor CS, Rajaraman S, Nichols TR, DeWeerth SP (2016) A stretchable microneedle electrode array for stimulating and measuring intramuscular electromyographic activity. IEEE Trans Neural Syst Rehabil Eng 25(9):1440–1452
18. Zhou W, Ling W-S, Liu W, Peng Y, Peng J (2015) Laser direct micromilling of copper-based bioelectrode with surface microstructure array. Opt Lasers Eng 73:7–15
19. Aoyagi S, Izumi H, Isono Y, Fukuda M, Ogawa H (2007) Laser fabrication of high aspect ratio thin holes on biodegradable polymer and its application to a microneedle. Sens Actuators, A 139(1–2):293–302
20. Omatsu T, Chujo K, Miyamoto K, Okida M, Nakamura K, Aoki N, Morita R (2010) Metal microneedle fabrication using twisted light with spin. Opt Express 18(17):17967–17973
21. Gill HS, Denson DD, Burris BA, Prausnitz MR (2008) Effect of microneedle design on pain in human subjects. Clin J Pain 24(7):585
22. Davis SP, Landis BJ, Adams ZH, Allen MG, Prausnitz MR (2004) Insertion of microneedles into skin: measurement and prediction of insertion force and needle fracture force. J Biomech 37(8):1155–1163
23. Fofonoff T, Wiseman C, Dyer R, Malasek J, Burgert J, Martel S, Hunter I, Hatsopoulos N, Donoghue J (2002) Mechanical assembly of a microelectrode array for use in a wireless intracortical recording device. *2nd Annual International IEEE-EMBS Special Topic Conference on Microtechnologies in Medicine and Biology*. Proceedings (Cat. No. 02EX578)
24. Vinayakumar KB, Rajanna K, Dinesh NS, Nayak MM (2016) Out-of-plane cup shaped stainless steel microneedle array for drug delivery. *In 2016 IEEE 11th Annual International Conference on Nano/Micro Engineered and Molecular Systems (NEMS)* (pp. 172–175). IEEE
25. Constantin CP, Aflori M, Damian RF, Rusu RD (2019) Biocompatibility of polyimides: a mini-review. Materials 12(19):3166
26. Larraneta E, Moore J, Vicente-Perez EM, Gonzalez-Vazquez P, Lutton R, Woolfson AD, Donnelly RF (2014) A proposed model membrane and test method for microneedle insertion studies. Int J Pharm 472(1–2):65–73. https://doi.org/10.1016/j.ijpharm.2014.05.042
27. Prausnitz MR (2017) Engineering microneedle patches for vaccination and drug delivery to skin. Annu Rev Chem Biomol Eng 8:177–200. https://doi.org/10.1146/annurev-chembioeng-060816-101514
28. Al-Qallaf B, Das DB (2009) Optimizing microneedle arrays to increase skin permeability for transdermal drug delivery. Ann N Y Acad Sci 1161(1):83–94

## Publisher's Note